

# Ginsenoside Rg3 induces mesangial cells proliferation and attenuates apoptosis by miR-216a-5p/MAPK pathway in diabetic kidney disease

Yuanzhen Chen<sup>1,\*</sup>, Yuhuan Peng<sup>2,\*</sup>, Ping Li<sup>1</sup>, Ying Jiang<sup>1</sup>, Dan Song<sup>1</sup>

<sup>1</sup>Department of Nephrology, Shenzhen Guangming District People's Hospital, Guangming, Shenzhen 518000, China

<sup>2</sup>Department of Pharmacy, Shenzhen Guangming District People's Hospital, Guangming, Shenzhen 518000, China

\*Equal contribution

**Correspondence to:** Dan Song; email: [songdancas@163.com](mailto:songdancas@163.com), <https://orcid.org/0000-0002-7970-5569>

**Keywords:** ginsenoside Rg3, diabetic nephropathy, miR-216a-5p, MAPK pathway, apoptosis

**Received:** January 31, 2024

**Accepted:** May 6, 2024

**Published:** June 7, 2024

**Copyright:** © 2024 Chen et al. This is an open access article distributed under the terms of the [Creative Commons Attribution License](https://creativecommons.org/licenses/by/4.0/) (CC BY 4.0), which permits unrestricted use, distribution, and reproduction in any medium, provided the original author and source are credited.

## ABSTRACT

**Background:** Ginsenoside Rg3 is an active saponin isolated from ginseng, which can reduce renal inflammation. However, the role and mechanism of Rg3 in diabetic kidney disease (DKD) are far from being studied.

**Methods:** The effects of Rg3 and miR-216a-5p on the proliferation, apoptosis, and MAPK pathway in high glucose (HG)-induced SV40 MES 13 were monitored by CCK-8, TUNEL staining, and western blot.

**Results:** Rg3 treatment could accelerate proliferation and suppress apoptosis in HG-induced SV40 MES. Moreover, miR-216a-5p inhibition also could alleviate renal injury, prevent apoptosis, and activate the MAPK pathway in kidney tissues of diabetic model mice.

**Conclusion:** Rg3 could attenuate DKD progression by downregulating miR-216a-5p, suggesting Rg3 and miR-216a-5p might be the potential drug and molecular targets for DKD therapy.

## INTRODUCTION

MicroRNA (miRNA) is a non-coding small molecule RNA of 21–24 nucleotides in length that can bind to mRNA through base complementary pairing to control the translation or degradation of the target mRNA [1]. Several studies have manifested that miRNAs can prevent or accelerate Diabetic kidney disease (DKD) progressions [2, 3]. miR-216a-5p is a member of the miRNA family, can attenuate the process of various diseases, such as cancer [4, 5], Alzheimer's disease [6], bronchopneumonia [7], neuropathic pain [8], etc. Additionally, research indicated that miR-216a-5p could induce HG-induced EMT and fibrogenesis by BMP7 in DKD [9]. However, the impact of miR-216a-5p on mesangial cell apoptosis remains unclear.

DKD as one of the major microvascular complications of diabetes, is now one of the leading causes of death in patients with end-stage renal disease (ESRD) [10].

Diabetes can cause multiple pathological structural changes in the kidney, such as vascular endothelial dysfunction, glomerular enlargement, thickening of the basement membrane, mesenchymal proliferation, and increased extracellular matrix [11, 12]. The clinical manifestations of DKD are the persistent decline of renal function, albuminuria, and edema [13]. Without intervention, it can progress to glomerulosclerosis, eventually leading to renal failure [14]. The occurrence of DKD is a long pathological process with complex mechanisms. Numerous clinical and experimental studies have suggested that inflammation is a key factor in the deterioration of renal function [15]. In the state of hyperglycemia, the inflammation of renal tissue is initiated through multiple signal pathways, among which the MAPK pathway is the most classical inflammatory pathway [16]. After activation, the MAPK pathway can phosphorylate different transcription factors, which can result in the production of inflammatory factors and participate in the inflammatory response of diseases

[17]. Therefore, it is vital to search for novel drugs and molecular targets that can block the activation of the MAPK pathway for DKD therapy.

Based on the characteristics of clinical manifestations, DKD can be classified into the categories of traditional Chinese medicine (TCM) “edema”, “deficiency”, and “Guange” [18]. It is mainly caused by spleen and kidney deficiency, dampness, and blood stasis block and is treated by invigorating the spleen and kidney and eliminating the turbid by purgation [19]. Ginseng is a rare TCM with a long history. It has the functions of enriching yin and nourishing kidney, invigorating spleen for benefiting lung, calming mind and enhancing intelligence [20, 21]. Ginsenoside is the main active component of ginseng, which also has anti-inflammatory, anti-microbial, antibacterial, anti-parasitic, anti-tumor, anti-virus, and other effects [22]. Ginsenoside Rg3 is a saponin compound in the TCM ginseng, which has a series of pharmacological activities such as alleviating inflammatory response, reducing oxygen free radicals, and anti-oxidation [23–25]. Studies manifested that Rg3 can alleviate the progression of DKD by enhancing antioxidant capacity, reducing inflammation, and anti-apoptosis [26, 27]. Rg3 can also attenuate high glucose (HG)-induced mesangial cell proliferation and inflammation by inhibiting NF- $\kappa$ B [26]. Besides, Research indicated that Rg3 can induce activated receptors and increase the activity of natural killer cells by the MAPK pathway [28]. Rg3 can restrain the proliferation of melanoma cells by weakening the MAPK pathway [29]. Rg3 can also induce angiogenesis in human endothelial cells through MAPK/ERK pathway [30]. These data suggested that Rg3 can induce the inactivation of the MAPK pathway. Therefore, further investigation of the effects of Rg3 on the MAPK pathway, renal histopathological injury, and apoptosis may provide a new experimental basis for the protective mechanism of Rg3 in renal tissue injury.

In our study, we constructed diabetic cell and mouse models and explored the influences of Rg3 on the proliferation and apoptosis in HG-treated SV40 MES and kidney tissues of diabetic model mice. Besides, we also explored the possible gene regulated by Rg3 in DKD progression and its effect on the MAPK pathway. Therefore, this study may provide a theoretical basis for the mechanism and clinical application of Rg3 in DKD.

## MATERIALS AND METHODS

### Cell culture, construction of diabetic model cells, and treatment

Mouse mesangial cells (SV40 MES 13) were purchased from ATCC (USA) and incubated in DMEM (Gibco,

USA) containing 10% fetal bovine serum (FBS, Gibco) and low sugar (5.5 mM) at 37°C and 5% CO<sub>2</sub>. Normal-cultured SV40 MES cells were disposed of with increasing concentrations of Rg3 (1, 2, 4, 6, 8, 16, and 32  $\mu$ M) for 48 h. To obtain diabetes model cells, SV40 MES 13 were incubated with DMEM including 30 mM glucose for 48 h [31]. miR-216a-5p mimics, miR-216a-5p inhibitors, and corresponding negative controls (NC) were acquired from GenePharma (Suzhou, China). And the high glucose (HG)-treated SV40 MES were treated with 2, 4, and 8  $\mu$ M Rg3 for 48 h. Besides, HG-treated SV40 MES were addressed with 8  $\mu$ M Rg3 and transfected with the miR-216a-5p mimics, inhibitor, or NC using Lipofectamine™ 3000 (Invitrogen, USA) for 48 h.

### Cell viability analysis

SV40 MES were inoculated into 96-well plates with  $2 \times 10^4$  cells/well and treated based on the research design. Then 10  $\mu$ l CCK-8 was added to each well and incubated for 2 h away from light. Absorbance at 450 nm was examined with a microplate reader, which was applied to evaluate the proliferation capacity.

### TUNEL staining

For cells, groups of SV40 MES were made into cell smears. After fixation with 4% paraformaldehyde (Sigma-Aldrich, USA), TUNEL staining and DAPI staining were performed. And the apoptotic cells were observed by a fluorescent microscope (Olympus IX71). For tissues, the kidney tissues mice were made into paraffin sections (3  $\mu$ m). Then the sections were dewaxed, dehydrated, dried, processed with trypsin K, added with the reaction solution, and incubated in a thermostat at 37°C for 1 h. After washing, the sections were stained with DAB, re-stained with hematoxylin, dehydrated with 75%, 80%, 95%, and 100% ethanol, and transparent with xylene. After sealing the sections with neutral gum, the sections were placed under a microscope for observation.

### Western blot

Total protein was extracted with RAPI lysate (Beyotime, China) from SV40 MES 13 or mouse kidney tissues, and the concentration was confirmed using a BCA kit. 30  $\mu$ g equal samples were separated by SDS-PAGE, then transferred to PVDF membrane (Millipore, USA), enclosed in 5% skim milk for 2 h. Then the membranes were exposed to primary antibodies including cle-Caspase 3 (Abcam, 1: 1000), cle-Caspase 8 (Abcam, 1: 500), Bcl2 (Abcam, 1: 500), Bax (Abcam, 1: 500), p-p70s6k (Abcam, 1: 500), p70s6k (Abcam, 1: 1000), p-MAPK (Abcam, 1: 500), MAPK (Abcam, 1: 1000) or

GAPDH (Abcam, 1: 2000) at 4°C overnight and secondary antibody for 2 h. After washing, the membrane was treated with ECL reagent (Millipore) and developed. Protein bands were analyzed by a Gel imaging System (Bio-Rad, USA). The gray value was analyzed using ImageJ Software. GAPDH served as a loading control.

### qRT-PCR

Total RNA was acquired from mouse kidney tissues or SV40 MES 13 by TRIzol (Invitrogen, USA). After the purity and concentration of RNA were qualified, cDNA was synthesized using a reverse transcription kit (Takara, Tokyo, Japan) based on the instructions. SYBR Green qPCR Master Mix (DBI Bioscience, China) was applied for the qRT-PCR analysis. And the level of miR-216a-5p was calculated by  $2^{-\Delta\Delta Ct}$ .

### Construction of diabetic model mice

Healthy SPF C57BL/6 mice (male, aged 6–7 weeks, weight 21–22 g) were purchased from Experimental Animal Center and fed in an SPF barrier system for one week at a constant temperature and given a 12:12 h circadian cycle of day and night, as well as clean food and drinking water. Then mice were randomly divided into a control group ( $n = 6$ ) and a model group ( $n = 18$ ). Mice in the model group were intraperitoneally injected with 50 mg/kg STZ (STZ dissolved in 0.1 mol/L sodium citrate buffer, pH4.5) for 5 consecutive days to establish a diabetes mouse model. The mice in the control group accepted the same volume of citrate buffer. Fasting blood glucose was measured by blood glucose meter after 7 d of modeling, and mice with blood glucose >16.7 mM after fasting were considered to be successfully modeled. The modeled mice were divided into 3 groups: diabetes model group (DKD,  $n = 6$ ), Rg3 administration group (DKD+Rg3, the mice were treated by oral gavage of the 20 mg/kg Rg3 for 8 weeks,  $n = 6$ ), and miR-216a-5p inhibitor group (DKD+inhibitor, the mice were injected with miR-216a-5p inhibitors through a tail vein for 3 days,  $n = 6$ ). The protocol was approved by the research ethics committees of the Shenzhen Guangming District People's Hospital (approval no. of ethics committee: LL-KT-2020075).

### H&E staining

Kidney tissue was fixed with 4% paraformaldehyde for 72 h, dehydrated by alcohol gradient, and embedded. Then the sections were cut into 4 μm by pathological microtome. After dewaxing and hydration, the sections were stained with H&E and sealed with neutral gum. The histological manifestation was observed with a microscope.

### Statistical analysis

All data were expressed as mean ± SD and analyzed by SPSS26.0 software with one-way ANOVA.  $P < 0.05$  was considered statistically significant.

## RESULTS

### Determination of Rg3 concentration in SV40 MES

To confirm the optimal concentration of Rg3 for treating SV40 MES. We applied different concentration gradients (0, 1, 2, 4, 8, 16, and 32 μM) of Rg3 to treat SV40 MES for 24 h. And the CCK-8 results demonstrated that the OD value in Rg3-treated SV40 MES 13 was notably ( $p < 0.001$ ) increased compared with the control group, and the proliferation capacity (OD value) of SV40 MES reached the peak when Rg3 concentration was 8 μM (Figure 1). Thus, 8 μM Rg3 was considered the optimal concentration for SV40 MES treatment.

### Rg3 treatment induces proliferation and prevents apoptosis in HG-induced SV40 MES

To investigate the mechanism of Rg3 in DKD, we constructed the DKD model of SV40 MES through 30 mM of HG treatment for 48 h. Then the HG-induced SV40 MES were addressed with 2, 4, and 8 μM Rg3. CCK-8 results suggested that the proliferation ability of SV40 MES 13 was markedly ( $p < 0.001$ ) reduced in the HG group relative to that in a control group, while Rg3 treatment could markedly improve the proliferation capacity of HG-induced SV40 MES 13 (Figure 2A). Meanwhile, the TUNEL data indicated that HG-induced apoptosis could be memorably ( $p < 0.001$ ) reversed after administration with Rg3 in SV40 MES 13 (Figure 2B, 2C). It was well known that up-regulation of cle-Caspase 3, cle-Caspase 8, and Bax expressions and downregulation of Bcl2 could expedite apoptosis. And our results exhibited that cle-Caspase 3, cle-Caspase 8, and Bax were distinctly ( $p < 0.001$ ) up-regulated, and Bcl2 was signally ( $p < 0.001$ ) decreased in HG-induced SV40 MES 13 relative to the control cells, while Rg3 could markedly reverse the expressions of these proteins in HG-induced SV40 MES 13 (Figure 2D).

### Rg3 induces proliferation, suppresses apoptosis, and activates the MAPK pathway by downregulating miR-216a-5p in HG-induced SV40 MES 13

Through literature analysis, we found that miR-216a-5p was highly expressed in HG-treated kidney cells [9]. And we also confirmed that miR-216a-5p expression was aggrandized in HG-induced SV40 MES 13, while Rg3 treatment dramatically ( $p < 0.001$ ) reversed the

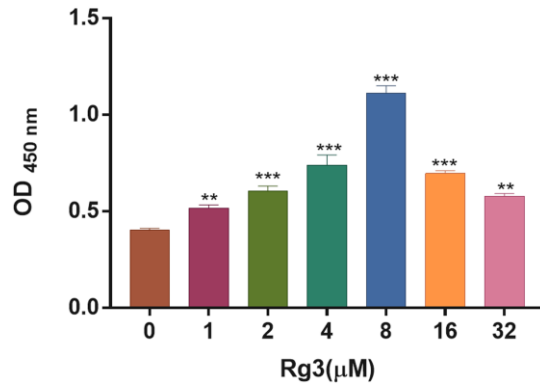


**Figure 1. Screening of appropriate Rg3 concentration in SV40 MES 13.** CCK-8 was conducted to confirm the change of cell proliferation in SV40 MES 13 after treating with 1, 2, 4, 8, 16, and 32 μM Rg3. \*\* $P < 0.01$ , \*\*\* $P < 0.001$ .

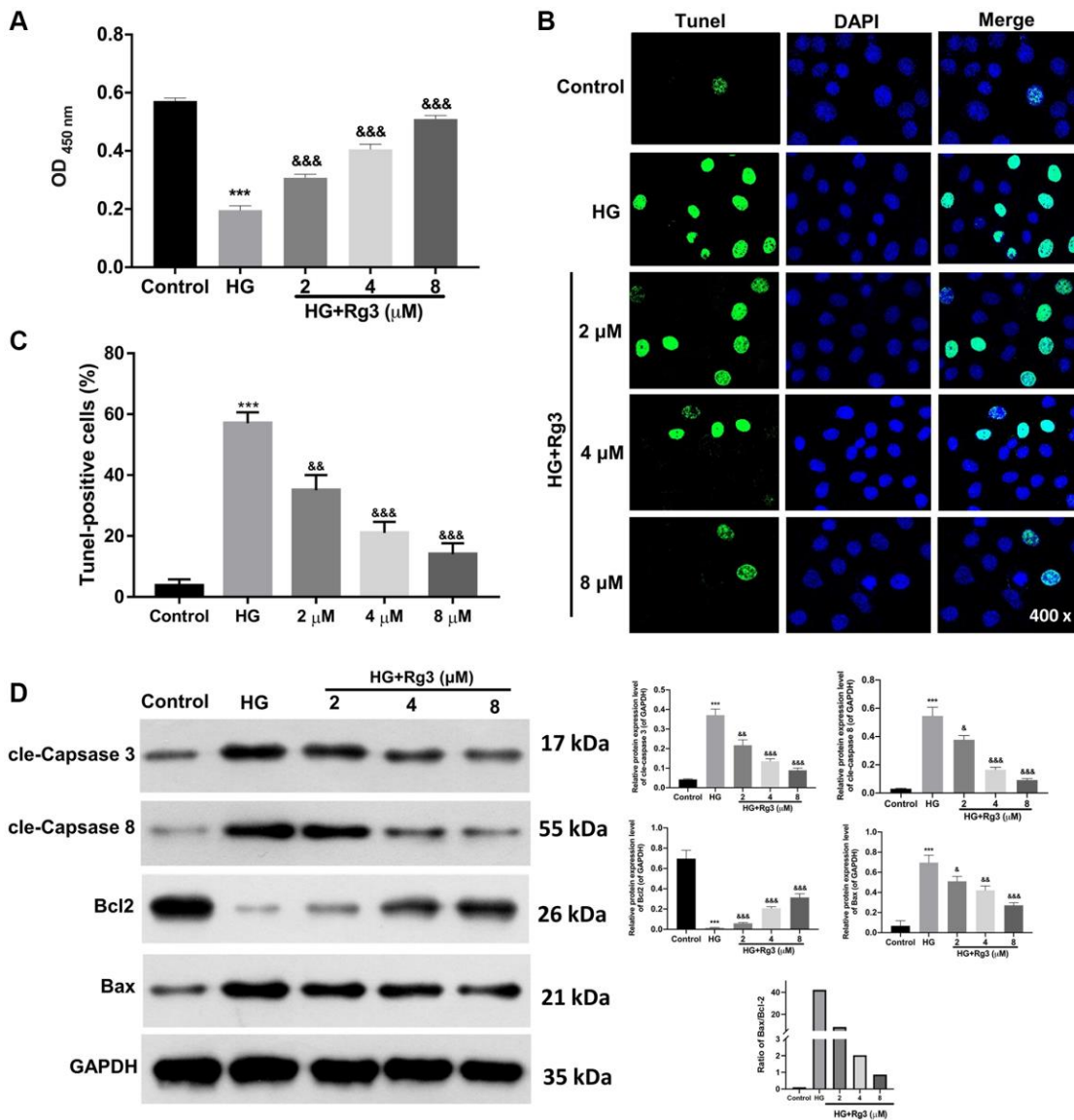


**Figure 2. Rg3 induces proliferation and prevents apoptosis in HG-induced SV40 MES 13.** HG-treated SV40 MES 13 were processed with 2, 4, and 8 μM Rg3. (A) Cell proliferation was monitored via CCK-8 in each group. (B) TUNEL analysis of cell apoptosis (Magnification, 200x). (C) Quantitative analysis of TUNEL results. (D) Western blot denoted the changes of cle-Capsase 3, cle-Capsase 8, Bcl2, and Bax expressions. \*\*\* $P < 0.001$  vs. control group; && $P < 0.01$  and &&& $P < 0.001$  vs. HG group.

upregulation of miR-216a-5p mediated by HG induction (Figure 3A). To further certify the mechanism of Rg3 and miR-216a-5p in DKD. HG-induced SV40 MES 13 cells were treated with miR-216a-5p inhibitors, mimics, and 8  $\mu$ M Rg3. qRT-PCR results revealed that miR-216a-5p was upregulated ( $p < 0.001$ ) in HG-induced SV40 MES

13, and miR-216a-5p inhibition downregulated miR-216a-5p, miR-216a-5p overexpression upregulated miR-216a-5p in HG-induced SV40 MES 13, and Rg3 also could reduce the upregulation of miR-216a-5p mediated by miR-216a-5p overexpression in HG-induced SV40 MES 13 (Figure 3B). Thus, we verified the successful

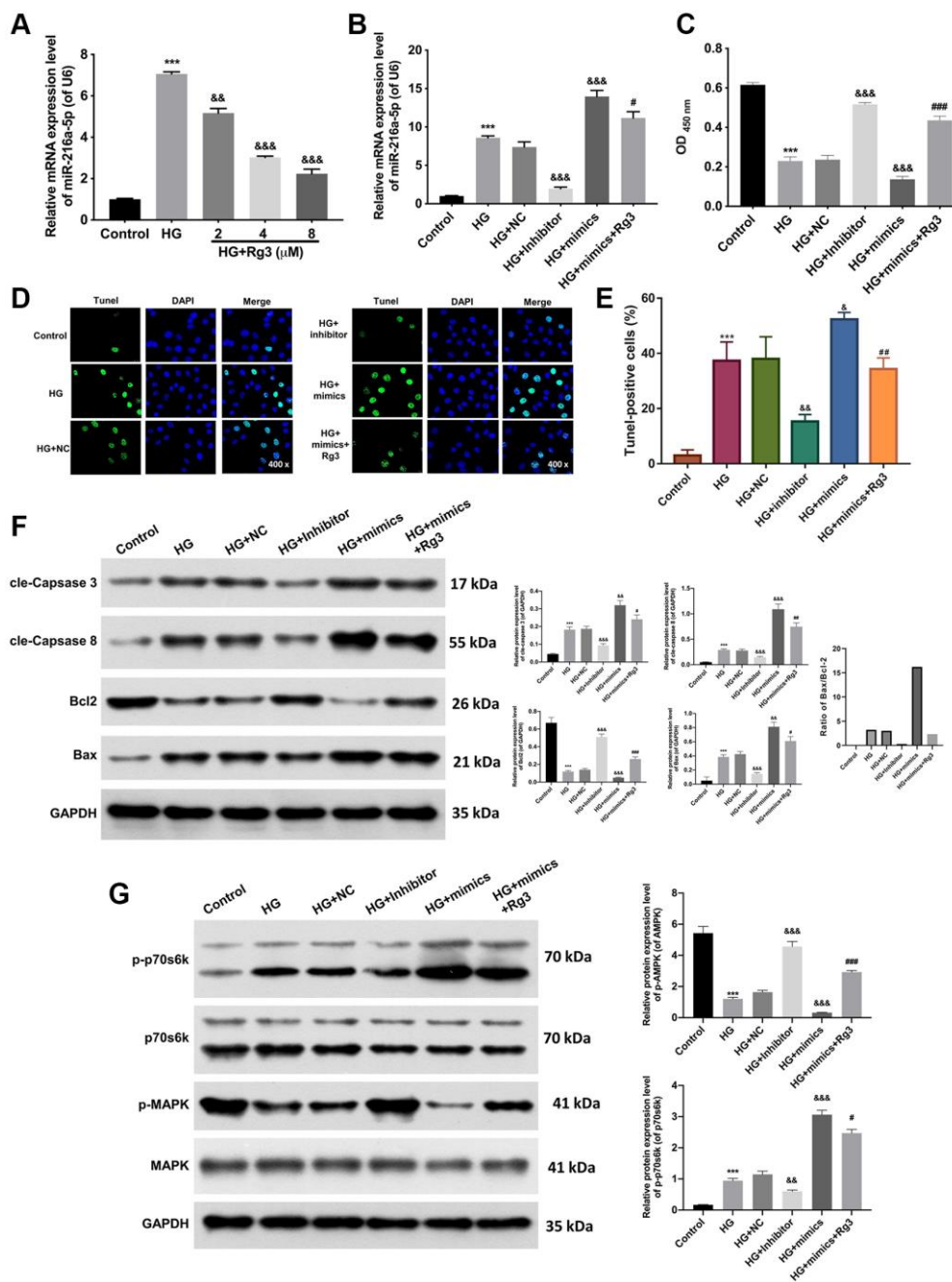


**Figure 3. Rg3 enhances proliferation, attenuates apoptosis, and activates the MAPK pathway through the downregulation of miR-216a-5p in HG-induced SV40 MES 13.** (A) qRT-PCR analysis for the evaluation of a miR-216a-5p expression in HG-induced SV40 MES 13 after processing with Rg3. (B) HG-induced SV40 MES 13 were transfected with miR-216a-5p inhibitor, miR-216a-5p mimics or NC, and treated with Rg3. The expression change of miR-216a-5p was identified by applying qRT-PCR. (C) CCK-8 assay for the examination of cell proliferation in SV40 MES 13 treated in the same way as B. (D) TUNEL staining revealed the change of cell apoptosis (Magnification, 200x). (E) TUNEL-positive cells were quantified. (F) The changes of cle-Capsase 3, cle-Capsase 8, Bcl2, and Bax expressions were confirmed through the application of western blot. (G) Western blot analysis of p-p70s6k, p70s6k, P-MAPK, and MAPK expressions in each group. \*\*\* $P < 0.001$  vs. control group; && $P < 0.01$ , &&& $P < 0.001$  vs. HG + NC group; # $P < 0.05$ , ## $P < 0.01$ , ### $P < 0.001$  vs. HG + mimics group.

transfection of miR-216a-5p inhibitors and miR-216a-5p mimics. Besides, CCK-8 displayed that inhibition of miR-216a-5p conspicuously ( $p < 0.001$ ) strengthened proliferation, overexpression of miR-216a-5p strikingly ( $p < 0.001$ ) weakened proliferation in HG-induced SV40 MES 13, while Rg3 notably ( $p < 0.001$ ) alleviated the attenuated effect of miR-216a-5p overexpression on cell proliferation in HG-induced SV40 MES 13 (Figure 3C). And TUNEL data revealed that miR-216a-5p inhibition distinctly restrained apoptosis and miR-216a-5p overexpression outstandingly ( $p < 0.001$ ) activated apoptosis, while Rg3 observably ( $p < 0.001$ ) attenuated the promoting effect of miR-216a-5p overexpression on the apoptosis of HG-induced SV40 MES 13 (Figure 3D, 3E). Moreover, western blot results presented that miR-216a-5p inhibition notably ( $p < 0.001$ ) downregulated cle-Caspase 3, cle-Caspase 8, and Bax, and upregulated ( $p < 0.001$ ) Bcl2 in HG-treated SV40 MES 13, and the effect of miR-216a-5p overexpression on these proteins was opposite to miR-216a-5p inhibition, and Rg3 also could outstandingly ( $p < 0.001$ ) reverse the upregulation of cle-Caspase 3, cle-Caspase 8, and Bax, and the downregulation of Bcl2 mediated by miR-216a-5p overexpression in HG-treated SV40 MES 13 (Figure 3F). Meanwhile, our data revealed that inhibition of miR-216a-5p memorably ( $p < 0.001$ ) downregulated p-p70s6k and upregulated p-MARK, and overexpression of miR-216a-5p prominently ( $p < 0.001$ ) upregulated p-p70s6k and downregulated p-MARK in HG-induced SV40 MES 13, while Rg3 also could markedly ( $p < 0.001$ ) attenuate the expression changes in p-p70s6k and p-MARK proteins mediated by miR-216a-5p overexpression in HG-treated SV40 MES 13 (Figure 3G).

### **Rg3 or miR-216a-5p inhibition ameliorates renal pathology, prevents apoptosis, and induces MAPK pathway in kidney tissues of diabetic model mice**

Moreover, we further assessed the mechanism of Rg3 in DKD through *in vivo* experiment. And a mouse diabetes model was built by feeding mice with STZ, and then the model mice were intragastric treated with 20 mg/kg Rg3 or injected with miR-216a-5p inhibitors. And the renal tissue was collected for a follow-up examination. qRT-PCR data revealed that miR-216a-5p was upregulated ( $p < 0.001$ ) in the renal tissues of DKD model mice relative to that in control mice, while Rg3 or miR-216a-5p inhibition prominently ( $p < 0.001$ ) attenuated the upregulation of miR-216a-5p in DKD model mice, especially miR-216a-5p inhibition (Figure 4A). And H&E staining results signified that in the control group, renal tissues were neatly aligned; in the DKD group, renal tissues showed typical glomerular injury, such as glomerulosclerosis, cellular vacuolization, basement membrane hyperplasia, and inflammatory cell infiltration; after Rg3 or miR-216a-5p inhibitor

intervention, renal injury damage and pro-inflammatory cell infiltration were reduced, and there was some degree of repair of the renal basement membrane (Figure 4B). Similarly, TUNEL results exhibited that the apoptotic capacity of renal tissues was markedly increased in DKD model mice, which also could be memorably attenuated by Rg3 treatment or miR-216a-5p inhibitor (Figure 4C). Besides, western blot results displayed that cle-Caspase 3, cle-Caspase 8 and Bax were conspicuously ( $p < 0.001$ ) upregulated, and Bcl2 was downregulated ( $p < 0.001$ ) in the renal tissues of DKD model mice, which also could be dramatically reversed by Rg3 treatment or miR-216a-5p inhibition, especially miR-216a-5p inhibition (Figure 4D). Then we also disclosed that Rg3 or miR-216a-5p inhibition could obviously ( $p < 0.001$ ) weakened the upregulation of p-p70s6k and downregulation of p-MARK in the renal tissues of DKD model mice, and the weakening effect of miR-216a-5p inhibition was more obvious ( $p < 0.001$ ) than that of Rg3 (Figure 4E). The blood glucose was measured (Figure 4F). Compared with DKD group, FBG levels were ( $p < 0.001$ ) significantly decreased in DKD+Rg3 and DKD+inhibitor group since the third week and continued to the end of this research. Renal measurements including blood urea nitrogen (BUN) and creatinine (Scr) were measured and shown in Figure 4G. We found that the levels of BUN and Scr were decreased significantly ( $p < 0.001$ ) in Rg3 and inhibitor treatment when compared with DKD group.

## **DISCUSSION**

The World Health Organization predicts that the number of people with diabetes will increase to 300 million worldwide by 2025 [32]. As the familiar complication of diabetes mellitus, DKD has become a crucial cause of chronic renal failure in the elderly [33]. The pathogenesis of DKD is complex and has not yet been fully understood. While studies have testified that metabolic disorders caused by persistent hyperglycemia are the leading cause of DKD [34]. Currently, Chinese herbs (astragalus, ginseng, and coptidis rhizome) have good hypoglycemic efficacy, and exhibit unique advantages in blood glucose control, such as multi-function, multi-target, low toxicity and side effects, safety and reliability, mild and long-lasting effects, which can effectively slow down the occurrence of DKD [35–37]. Ginseng, as a TCM, is useful in the prevention and therapy of numerous diseases. Among them, ginsenoside Rg3 is mainly discovered in the root of ginseng, which belongs to the phytosterols of natural products. Rg3 has various pharmacological effects, such as anti-tumor, anti-cardiovascular disease, antidepressant, anti-inflammatory, and neuroprotection, and can regulate multiple signal transduction pathways and molecular targets [24, 38]. In the streptozotocin

(STZ)-induced DKD rat model, Rg3 was also proved to protect the kidney by reducing oxidative stress and apoptosis [26, 27]. In this study, we also revealed that Rg3 has an inducing effect on proliferation and a blocking effect on apoptosis in HG-induced SV40 MES 13. Moreover, Rg3 also could ameliorate renal injury

and weaken apoptosis of kidney tissues in diabetic model mice. Thus, we suggested that Rg3 has a significant protective effect on DKD.

Whether Rg3 can play a protective role on DKD by regulating miR-216a-5p has not been reported. In the

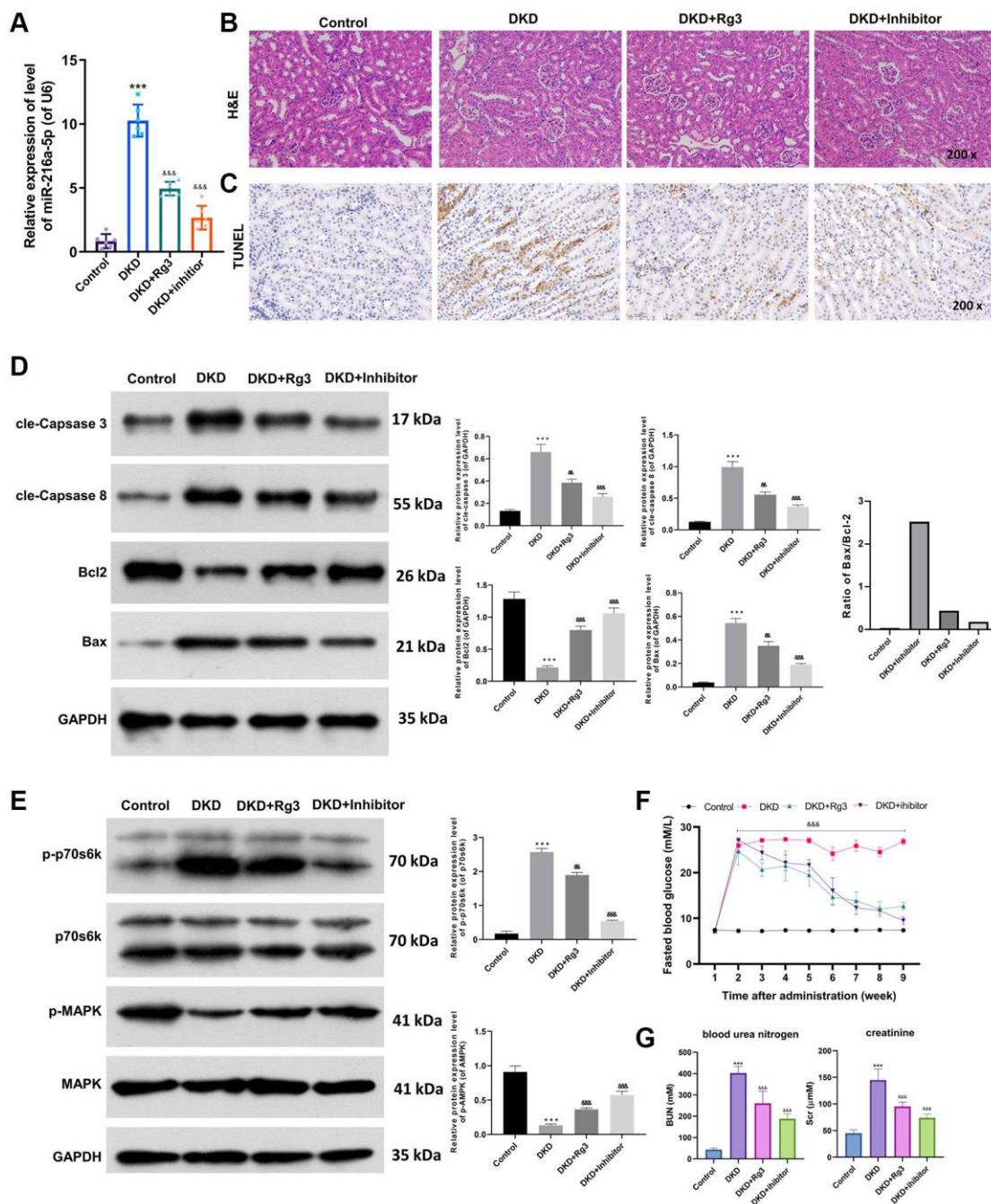


**Figure 4. Rg3 or miR-216a-5p inhibition alleviates kidney injury, prevents apoptosis, and induces MAPK pathway in kidney tissues of diabetic model mice.** And we first fed mice with STZ to build a mouse diabetes model, and then treated by oral gavage of the 20 mg/kg Rg3 for 8 weeks or injected with miR-216a-5p inhibitors through a tail vein (once a day for 3 days). (A) qRT-PCR was adopted to assess the change of miR-216a-5p in the mice kidney tissues. (B) H&E staining indicated the pathological change of kidney tissues (Magnification, 200×). (C) TUNEL staining for the confirmation of cell apoptosis (Magnification, 200×). (D) Western blot was applied to analyze the expression changes of apoptosis-related proteins. (E) Western blot showed the changes of p-p70s6k, p70s6k, p-MAPK, and MAPK expressions. (F) Fasting blood glucose. (G) Blood urea nitrogen and creatinine. \*\*\* $P < 0.001$  vs. control group; &&P < 0.01, &&&P < 0.001 vs. DKD group.

current study, we confirmed that Rg3 could accelerate proliferation and restrain apoptosis by downregulating miR-216a-5p in HG-induced SV40 MES 13. Meanwhile, similar to Rg3, miR-216a-5p inhibition also could improve the pathological damage of the kidney and prevent apoptosis of kidney tissues in diabetic model mice. Thus, we also proved that miR-216a-5p inhibition also has a protective effect on DKD.

The occurrence of DKD involves diverse and complex cellular pathways, such as the MAPK pathway [1]. MAPK is a vital member of the MAPK family. High glucose can induce the activation of MAPK [39, 40]. Research showed that MAPK can promote cell proliferation, cause renal hypertrophy, glomerulosclerosis [41]. In recent years, researches also proved that some Chinese herbs (such as chlorogenic acid, apigenin, Huangkui capsule) have inhibitory effects on MAPK activity and can effectively reduce or even prevent the occurrence of DKD [42–44]. Studies also demonstrated that Rg3 can induce the activation of the MAPK pathway [28, 30]. In our study, we also revealed that Rg3 could activate the MAPK pathway by downregulating miR-216a-5p in HG-induced SV40 MES 13, and Rg3 or miR-216a-5p inhibition also could induce the MAPK pathway in kidney tissues of diabetic model mice. We initially revealed that Rg3 could prevent the development of DKD by downregulating miR-216a-5p and activating MAPK pathway. However, the specific mechanism still needs further verification.

In summary, ginsenoside Rg3 can suppress the apoptosis of renal tissue cells, leading to renal injury in DKD mice, and its mechanism may be relevant to the inhibition of miR-216a-5p.

## AUTHOR CONTRIBUTIONS

Yuanzhen Chen and Yuhuan Peng: designed and performed research, as well as collected, analyzed, interpreted results and writing. Ping Li and Ying Jiang: helped performed some experiments. Dan Song: obtained funding for the project, initiated and supervised the project, designed research, analyzed and interpreted results, and revised the manuscript. All authors reviewed the results and approved the final version of the manuscript, All the authors contributed substantially to the manuscript.

## CONFLICTS OF INTEREST

The authors declare no conflicts of interest related to this study.

## ETHICAL STATEMENT

This study was approved by the Ethics Committee of The Shenzhen Guangming District People's Hospital

(approval no. of ethics committee: LL-KT-2020075). All applicable international, national, and/or institutional guidelines for the care and use of animals were followed.

## FUNDING

This work is supported by Project supported by the Guangming District Economic Development Special Fund (2020R01129).

## REFERENCES

1. Ho PTB, Clark IM, Le LTT. MicroRNA-Based Diagnosis and Therapy. *Int J Mol Sci.* 2022; 23:7167. <https://doi.org/10.3390/ijms23137167> PMID:[35806173](https://pubmed.ncbi.nlm.nih.gov/35806173/)
2. He M, Wang J, Yin Z, Zhao Y, Hou H, Fan J, Li H, Wen Z, Tang J, Wang Y, Wang DW, Chen C. MiR-320a induces diabetic nephropathy via inhibiting MafB. *Aging (Albany NY).* 2019; 11:3055–79. <https://doi.org/10.18632/aging.101962> PMID:[31102503](https://pubmed.ncbi.nlm.nih.gov/31102503/)
3. Li Y, Xu Y, Hou Y, Li R. Construction and Bioinformatics Analysis of the miRNA-mRNA Regulatory Network in Diabetic Nephropathy. *J Healthc Eng.* 2021; 2021:8161701. <https://doi.org/10.1155/2021/8161701> PMID:[34840704](https://pubmed.ncbi.nlm.nih.gov/34840704/). Retraction in: *J Healthc Eng.* 2023; 2023:9858642. <https://doi.org/10.1155/2023/9858642> PMID:[37886319](https://pubmed.ncbi.nlm.nih.gov/37886319/)
4. Zhang J, Gao S, Zhang Y, Yi H, Xu M, Xu J, Liu H, Ding Z, He H, Wang H, Hao Z, Sun L, Liu Y, Wei F. MiR-216a-5p inhibits tumorigenesis in Pancreatic Cancer by targeting TPT1/mTORC1 and is mediated by LINC01133. *Int J Biol Sci.* 2020; 16:2612–27. <https://doi.org/10.7150/ijbs.46822> PMID:[32792860](https://pubmed.ncbi.nlm.nih.gov/32792860/)
5. Zhang Y, Lin P, Zou JY, Zou G, Wang WZ, Liu YL, Zhao HW, Fang AP. MiR-216a-5p act as a tumor suppressor, regulating the cell proliferation and metastasis by targeting PAK2 in breast cancer. *Eur Rev Med Pharmacol Sci.* 2019; 23:2469–75. [https://doi.org/10.26355/eurrev\\_201903\\_17394](https://doi.org/10.26355/eurrev_201903_17394) PMID:[30964173](https://pubmed.ncbi.nlm.nih.gov/30964173/)
6. Shao P. MiR-216a-5p ameliorates learning-memory deficits and neuroinflammatory response of Alzheimer's disease mice via regulation of HMGB1/NF- $\kappa$ B signaling. *Brain Res.* 2021; 1766:147511. <https://doi.org/10.1016/j.brainres.2021.147511> PMID:[33957091](https://pubmed.ncbi.nlm.nih.gov/33957091/)
7. Liu S, Li J, Hu L. MiR-216a-5p alleviates LPS-induced inflammation in the human bronchial epithelial cell by

- inhibition of TGF- $\beta$ 1 signaling via down-regulating TGFBR2. *Allergol Immunopathol (Madr)*. 2021; 49:64–71. <https://doi.org/10.15586/aei.v49i5.458> PMID:34476924
8. Wang W, Li R. MiR-216a-5p alleviates chronic constriction injury-induced neuropathic pain in rats by targeting KDM3A and inactivating Wnt/ $\beta$ -catenin signaling pathway. *Neurosci Res*. 2021; 170:255–64. <https://doi.org/10.1016/j.neures.2020.08.001> PMID:32889066
  9. Meng Q, Zhai X, Yuan Y, Ji Q, Zhang P. lncRNA ZEB1-AS1 inhibits high glucose-induced EMT and fibrogenesis by regulating the miR-216a-5p/BMP7 axis in diabetic nephropathy. *Braz J Med Biol Res*. 2020; 53:e9288. <https://doi.org/10.1590/1414-431X20209288> PMID:32294702. Retraction in: *Braz J Med Biol Res*. 2023; 56:e9288. <https://doi.org/10.1590/1414-431X2023e9288retraction> PMID:37194836
  10. Samsu N. Diabetic Nephropathy: Challenges in Pathogenesis, Diagnosis, and Treatment. *Biomed Res Int*. 2021; 2021:1497449. <https://doi.org/10.1155/2021/1497449> PMID:34307650
  11. Brosius FC, Coward RJ. Podocytes, signaling pathways, and vascular factors in diabetic kidney disease. *Adv Chronic Kidney Dis*. 2014; 21:304–10. <https://doi.org/10.1053/j.ackd.2014.03.011> PMID:24780459
  12. Chagnac A, Zingerman B, Rozen-Zvi B, Herman-Edelstein M. Consequences of Glomerular Hyperfiltration: The Role of Physical Forces in the Pathogenesis of Chronic Kidney Disease in Diabetes and Obesity. *Nephron*. 2019; 143:38–42. <https://doi.org/10.1159/000499486> PMID:30947190
  13. Tervaert TW, Mooyaart AL, Amann K, Cohen AH, Cook HT, Drachenberg CB, Ferrario F, Fogo AB, Haas M, de Heer E, Joh K, Noël LH, Radhakrishnan J, et al, and Renal Pathology Society. Pathologic classification of diabetic nephropathy. *J Am Soc Nephrol*. 2010; 21:556–63. <https://doi.org/10.1681/ASN.2010010010> PMID:20167701
  14. Vaidya SR, Aeddula NR. Chronic renal failure. StatPearls. StatPearls Publishing. 2021.
  15. Li X, Lu L, Hou W, Huang T, Chen X, Qi J, Zhao Y, Zhu M. Epigenetics in the pathogenesis of diabetic nephropathy. *Acta Biochim Biophys Sin (Shanghai)*. 2022; 54:163–72. <https://doi.org/10.3724/abbs.2021016> PMID:35130617
  16. Rane MJ, Song Y, Jin S, Barati MT, Wu R, Kausar H, Tan Y, Wang Y, Zhou G, Klein JB, Li X, Cai L. Interplay between Akt and p38 MAPK pathways in the regulation of renal tubular cell apoptosis associated with diabetic nephropathy. *Am J Physiol Renal Physiol*. 2010; 298:F49–61. <https://doi.org/10.1152/ajprenal.00032.2009> PMID:19726550
  17. Yong HY, Koh MS, Moon A. The p38 MAPK inhibitors for the treatment of inflammatory diseases and cancer. *Expert Opin Investig Drugs*. 2009; 18:1893–905. <https://doi.org/10.1517/13543780903321490> PMID:19852565
  18. An X, Fan D, Yin Z, Zhang J, Zhou Y, Tian R, Yan M. Prediction of the Potential Mechanism of Triptolide in Improving Diabetic Nephropathy by Utilizing A Network Pharmacology and Molecular Docking Approach. *Front Biosci (Landmark Ed)*. 2022; 27:94. <https://doi.org/10.31083/j.fbl2703094> PMID:35345326
  19. Lu Z, Zhong Y, Liu W, Xiang L, Deng Y. The Efficacy and Mechanism of Chinese Herbal Medicine on Diabetic Kidney Disease. *J Diabetes Res*. 2019; 2019:2697672. <https://doi.org/10.1155/2019/2697672> PMID:31534972
  20. Arring NM, Millstine D, Marks LA, Nail LM. Ginseng as a Treatment for Fatigue: A Systematic Review. *J Altern Complement Med*. 2018; 24:624–33. <https://doi.org/10.1089/acm.2017.0361> PMID:29624410
  21. Chen W, Balan P, Popovich DG. Review of Ginseng Anti-Diabetic Studies. *Molecules*. 2019; 24:4501. <https://doi.org/10.3390/molecules24244501> PMID:31835292
  22. Chen YY, Liu QP, An P, Jia M, Luan X, Tang JY, Zhang H. Ginsenoside Rd: A promising natural neuroprotective agent. *Phytomedicine*. 2022; 95:153883. <https://doi.org/10.1016/j.phymed.2021.153883> PMID:34952508
  23. Li L, Wang Y, Guo R, Li S, Ni J, Gao S, Gao X, Mao J, Zhu Y, Wu P, Wang H, Kong D, Zhang H, et al. Ginsenoside Rg3-loaded, reactive oxygen species-responsive polymeric nanoparticles for alleviating myocardial ischemia-reperfusion injury. *J Control Release*. 2020; 317:259–72. <https://doi.org/10.1016/j.jconrel.2019.11.032> PMID:31783047
  24. Nakhjavani M, Smith E, Townsend AR, Price TJ, Hardingham JE. Anti-Angiogenic Properties of Ginsenoside Rg3. *Molecules*. 2020; 25:4905.

- <https://doi.org/10.3390/molecules25214905>  
PMID:[33113992](https://pubmed.ncbi.nlm.nih.gov/33113992/)
25. Zhu Y, Liang J, Gao C, Wang A, Xia J, Hong C, Zhong Z, Zuo Z, Kim J, Ren H, Li S, Wang Q, Zhang F, Wang J. Multifunctional ginsenoside Rg3-based liposomes for glioma targeting therapy. *J Control Release*. 2021; 330:641–57.  
<https://doi.org/10.1016/j.jconrel.2020.12.036>  
PMID:[33359582](https://pubmed.ncbi.nlm.nih.gov/33359582/)
26. Li Y, Hou JG, Liu Z, Gong XJ, Hu JN, Wang YP, Liu WC, Lin XH, Wang Z, Li W. Alleviative effects of 20(R)-Rg3 on HFD/STZ-induced diabetic nephropathy via MAPK/NF- $\kappa$ B signaling pathways in C57BL/6 mice. *J Ethnopharmacol*. 2021; 267:113500.  
<https://doi.org/10.1016/j.jep.2020.113500>  
PMID:[33091499](https://pubmed.ncbi.nlm.nih.gov/33091499/)
27. Zhou T, Sun L, Yang S, Lv Y, Cao Y, Gang X, Wang G. 20(S)-Ginsenoside Rg3 Protects Kidney from Diabetic Kidney Disease via Renal Inflammation Depression in Diabetic Rats. *J Diabetes Res*. 2020; 2020:7152176.  
<https://doi.org/10.1155/2020/7152176>  
PMID:[32258169](https://pubmed.ncbi.nlm.nih.gov/32258169/)
28. Lee Y, Park A, Park YJ, Jung H, Kim TD, Noh JY, Choi I, Lee S, Ran Yoon S. Ginsenoside 20(R)-Rg3 enhances natural killer cell activity by increasing activating receptor expression through the MAPK/ERK signaling pathway. *Int Immunopharmacol*. 2022; 107:108618.  
<https://doi.org/10.1016/j.intimp.2022.108618>  
PMID:[35219164](https://pubmed.ncbi.nlm.nih.gov/35219164/)
29. Shan X, Aziz F, Tian LL, Wang XQ, Yan Q, Liu JW. Ginsenoside Rg3-induced EGFR/MAPK pathway deactivation inhibits melanoma cell proliferation by decreasing FUT4/LeY expression. *Int J Oncol*. 2015; 46:1667–76.  
<https://doi.org/10.3892/ijo.2015.2886>  
PMID:[25672851](https://pubmed.ncbi.nlm.nih.gov/25672851/)
30. Choi RJ, Mohamad Zobir SZ, Alexander-Dann B, Sharma N, Ma MKL, Lam BYH, Yeo GSH, Zhang W, Fan TP, Bender A. Combination of Ginsenosides Rb2 and Rg3 Promotes Angiogenic Phenotype of Human Endothelial Cells via PI3K/Akt and MAPK/ERK Pathways. *Front Pharmacol*. 2021; 12:618773.  
<https://doi.org/10.3389/fphar.2021.618773>  
PMID:[33643049](https://pubmed.ncbi.nlm.nih.gov/33643049/)
31. Du Y, Yang YT, Tang G, Jia JS, Zhu N, Yuan WJ. Butyrate alleviates diabetic kidney disease by mediating the miR-7a-5p/P311/TGF- $\beta$ 1 pathway. *FASEB J*. 2020; 34:10462–75.  
<https://doi.org/10.1096/fj.202000431R>  
PMID:[32539181](https://pubmed.ncbi.nlm.nih.gov/32539181/)
32. Hajam YA, Rani R, Malik JA, Pandita A, Sharma R, Kumar R. Diabetes Mellitus: Signs and Symptoms, Epidemiology, Current Prevention, Management Therapies, and Treatments. *Antidiabetic Potential of Plants in the Era of Omics*. Apple Academic Press. 2023; 31–77.
33. Umanath K, Lewis JB. Update on Diabetic Nephropathy: Core Curriculum 2018. *Am J Kidney Dis*. 2018; 71:884–95.  
<https://doi.org/10.1053/j.ajkd.2017.10.026>  
PMID:[29398179](https://pubmed.ncbi.nlm.nih.gov/29398179/)
34. Sagoo MK, Gnudi L. Diabetic Nephropathy: An Overview. *Methods Mol Biol*. 2020; 2067:3–7.  
[https://doi.org/10.1007/978-1-4939-9841-8\\_1](https://doi.org/10.1007/978-1-4939-9841-8_1)  
PMID:[31701441](https://pubmed.ncbi.nlm.nih.gov/31701441/)
35. Dong Y, Zhao Q, Wang Y. Network pharmacology-based investigation of potential targets of astragalus membranaceous-angelica sinensis compound acting on diabetic nephropathy. *Sci Rep*. 2021; 11:19496.  
<https://doi.org/10.1038/s41598-021-98925-6>  
PMID:[34593896](https://pubmed.ncbi.nlm.nih.gov/34593896/)
36. Bai L, Gao J, Wei F, Zhao J, Wang D, Wei J. Therapeutic Potential of Ginsenosides as an Adjuvant Treatment for Diabetes. *Front Pharmacol*. 2018; 9:423.  
<https://doi.org/10.3389/fphar.2018.00423>  
PMID:[29765322](https://pubmed.ncbi.nlm.nih.gov/29765322/)
37. Liu S, Chen XQ, Tang LQ, Yu N, Zhang XL, Du HF. [Regulatory effect of compound Coptidis Rhizoma capsule on unbalanced expression of renal tissue TGF- $\beta$ 1/BMP-7 and Smad signaling pathway in rats with early diabetic nephropathy]. *Zhongguo Zhong Yao Za Zhi*. 2015; 40:938–45.  
PMID:[26087560](https://pubmed.ncbi.nlm.nih.gov/26087560/)
38. Sun M, Ye Y, Xiao L, Duan X, Zhang Y, Zhang H. Anticancer effects of ginsenoside Rg3 (Review). *Int J Mol Med*. 2017; 39:507–18.  
<https://doi.org/10.3892/ijmm.2017.2857>  
PMID:[28098857](https://pubmed.ncbi.nlm.nih.gov/28098857/)
39. Guo YJ, Pan WW, Liu SB, Shen ZF, Xu Y, Hu LL. ERK/MAPK signalling pathway and tumorigenesis. *Exp Ther Med*. 2020; 19:1997–2007.  
<https://doi.org/10.3892/etm.2020.8454>  
PMID:[32104259](https://pubmed.ncbi.nlm.nih.gov/32104259/)
40. Yong J, Groeger S, Meyle J, Ruf S. MAPK and  $\beta$ -Catenin signaling: implication and interplay in orthodontic tooth movement. *Front Biosci (Landmark Ed)*. 2022; 27:54.  
<https://doi.org/10.31083/j.fbl2702054>  
PMID:[35226997](https://pubmed.ncbi.nlm.nih.gov/35226997/)
41. Hung PH, Hsu YC, Chen TH, Lin CL. Recent Advances in Diabetic Kidney Diseases: From Kidney Injury to Kidney Fibrosis. *Int J Mol Sci*. 2021; 22:11857.

<https://doi.org/10.3390/ijms222111857>

PMID:[34769288](https://pubmed.ncbi.nlm.nih.gov/34769288/)

42. Tzeng TF, Liou SS, Chang CJ, Liu IM. The ethanol extract of *Lonicera japonica* (Japanese honeysuckle) attenuates diabetic nephropathy by inhibiting p-38 MAPK activity in streptozotocin-induced diabetic rats. *Planta Med.* 2014; 80:121–9.  
<https://doi.org/10.1055/s-0033-1360196>  
PMID:[24431014](https://pubmed.ncbi.nlm.nih.gov/24431014/)
43. Malik S, Suchal K, Khan SI, Bhatia J, Kishore K, Dinda AK, Arya DS. Apigenin ameliorates streptozotocin-induced diabetic nephropathy in rats via MAPK-NF- $\kappa$ B-TNF- $\alpha$  and TGF- $\beta$ 1-MAPK-fibronectin pathways. *Am J Physiol Renal Physiol.* 2017; 313:F414–22.  
<https://doi.org/10.1152/ajprenal.00393.2016>  
PMID:[28566504](https://pubmed.ncbi.nlm.nih.gov/28566504/)
44. Mao ZM, Shen SM, Wan YG, Sun W, Chen HL, Huang MM, Yang JJ, Wu W, Tang HT, Tang RM. Huangkui capsule attenuates renal fibrosis in diabetic nephropathy rats through regulating oxidative stress and p38MAPK/Akt pathways, compared to  $\alpha$ -lipoic acid. *J Ethnopharmacol.* 2015; 173:256–65.  
<https://doi.org/10.1016/j.jep.2015.07.036>  
PMID:[26226437](https://pubmed.ncbi.nlm.nih.gov/26226437/)